



Spatiotemporal characteristics of precipitation diurnal variations in Chongqing with complex terrain

Shaoying Chen¹ · Yan Yan¹ · Gang Liu¹ · Dexian Fang² · Zheng Wu² · Jun He³ · Jianping Tang¹

Received: 21 November 2017 / Accepted: 8 October 2018 / Published online: 16 October 2018
© Springer-Verlag GmbH Austria, part of Springer Nature 2018

Abstract

Using the hourly precipitation data observed at 34 gauge stations in Chongqing during 1991–2012, the spatial and temporal characteristics of the precipitation amount (PA), precipitation intensity (PI), precipitation frequency (PF), and their diurnal cycles are analyzed. Results show that the PA increased from the western to eastern Chongqing in spring and autumn. The summer precipitation was dominant throughout the year, and the PA in the basin was larger than in the eastern and middle mountainous area, which was different from in spring and autumn. The nocturnal precipitation had a quasi-stationary feature. The diurnal peaks of the PA/PI/PF mainly appeared from midnight to early morning. The amplitude of the PF was significantly greater than that of the PI and thus determined the characteristics of diurnal variation of the PA. In terms of the distribution of peak time of precipitation, this study reveals a time lag indicating the peak time was later in the northeast than in the southwest Chongqing. The complex terrain played an important role in the difference of diurnal cycle of precipitation in different areas. The stations in the southwest Chongqing are largely located in the Sichuan Basin, while the stations in the eastern and middle Chongqing are located in the mountainous area surrounding the basin. By selecting 16 representative stations in two types of terrain for analysis, it is shown in the study that the amplitude of diurnal precipitation at the stations in higher terrain was weaker. Moreover, investigating the interval of precipitation associated with the diurnal distribution of lightning reveals that the enhancement of precipitation in the mountainous area in the afternoon was mainly caused by the short-time strong rainfall resulting from the convection.

1 Introduction

The spatial and temporal characteristics of diurnal variation of precipitation play an important role in revealing the changes of soil moisture, sensible and latent heat on the earth's surface and in the atmosphere. They are also implicated with hydrology and meteorology, especially with natural disasters such as extreme precipitation. Research

on the characteristics of diurnal variation of precipitation can help us understand the physical mechanism of precipitation and verify and improve precipitation parameterization schemes in numerical models.

Many studies have analyzed the characteristics of diurnal variation of precipitation over East Asian monsoon region with hourly gauge-observed precipitation data and satellite precipitation data (Yu et al. 2014a, b; Li et al. 2016). Yu et al. (2007) used the gauge observation data at 588 stations from 1991 to 2004 to analyze the diurnal variations of the summer precipitation in China, and found some significant regional differences. He and Zhang (2010) studied the diurnal cycle of precipitation in the warm season in northern China using the precipitation data of CMORPH satellite. Bao et al. (2011) also used the precipitation data of CMORPH satellite to study the characteristics of diurnal variation of the warm season precipitation over the eastern Tibetan Plateau. Chen et al. (2012a) used the gauge precipitation data and TRMM satellite data to study the diurnal variation of precipitation in the southeast Tibetan Plateau, trying to explain the distribution of diurnal variation of precipitation with topography. Based on

✉ Gang Liu
gangliu@nju.edu.cn

✉ Jianping Tang
jptang@nju.edu.cn

¹ CMA-NJU Joint Laboratory for Climate Prediction Studies, Institute for Climate and Global Change Research, School of Atmospheric Sciences, Nanjing University, Xianlin Campus, 163 Xianlin Road, Nanjing, China

² Chongqing Institute of Meteorological Sciences, Chongqing, China

³ Chongqing Meteorological Observatory, Chongqing, China

the hourly gauge precipitation data, Zhuo et al. (2014) analyzed the diurnal variation of precipitation in Shandong province and discussed regional differences as well as the propagation characteristics of precipitation with high time-resolution gauge data.

Due to the forcing effect of complex terrain, the diurnal variation of precipitation has very strong regional differences. Terrain has very important influences on the formation of precipitation and its characteristics of diurnal variation. Using high resolution radar data, Mandapaka et al. (2013) studied the diurnal cycle of precipitation over the Alps and surrounding complex terrain in terms of different season, region, interannual change, and vertical structure. The terrain altitude of China changes significantly from low in the east to high in the west, while different regions have their unique topography. Liu and Ma (2013) analyzed the diurnal difference of precipitation in China, finding a difference between the east and west. The southwest was dominated by the nighttime precipitation, while the east by the daytime precipitation. Zhang et al. (2014) compared precipitation propagation between in the east Tibetan Plateau and in the downstream of the Rocky Mountains, focusing on the similarities and differences of diurnal variation of precipitation caused by large topography. Chen et al. (2012b) analyzed the diurnal cycle of the warm season precipitation with gauge precipitation data over the southeast Tibetan Plateau, thinking local circulation may have caused the difference of diurnal variation of precipitation in this area. In terms of the special terrains in the Tibetan plateau, Yunnan-Guizhou Plateau, and Sichuan Basin, Qian et al. (2015) analyzed the diurnal variation of precipitation in these

areas and thought the reason for the characteristics of diurnal variation was the joint effects of multiple local circulations caused by the topographic contrasts.

Although the researches on the diurnal variation of precipitation over complex terrain have made significant progresses, there are still many problems that need to be further studied. They include (1) the gauge stations used by previous researches were relatively sparse, which could not reflect the topographic features; (2) the data of precipitation were short in temporal length, even only for a few years; and (3) there have not been ample researches on the interannual and interdecadal characteristics of diurnal variation of precipitation, especially over complex terrain. Moreover, the analysis of diurnal variation of long-term precipitation data can help us understand local climate characteristics. Further, based on application of lightning data to the study on the diurnal variation of precipitation (Tapia et al. 1998; Gungler and Krider 2006; Liu and Zipser 2008; Hyun et al. 2010), high-density lightning data can be used to analyze the spatial and temporal characteristics of diurnal variation of precipitation over complex terrain.

Chongqing is located in an inland area spanning $105^{\circ} 11' \sim 110^{\circ} 11' \text{ E}$ and $28^{\circ} 10' \sim 32^{\circ} 13' \text{ N}$ in the eastern Sichuan Basin in the southwest China. It is in the middle and upper reaches of the Yangtze River in the sub-tropical climate zone affected by the Tibetan Plateau significantly. The topographic features of Chongqing are complex. The west Chongqing goes deep into the Sichuan Basin while the east Chongqing gradually raises eastward and reaches the edge of the Sichuan Basin. Studying the precipitation in Chongqing is important to

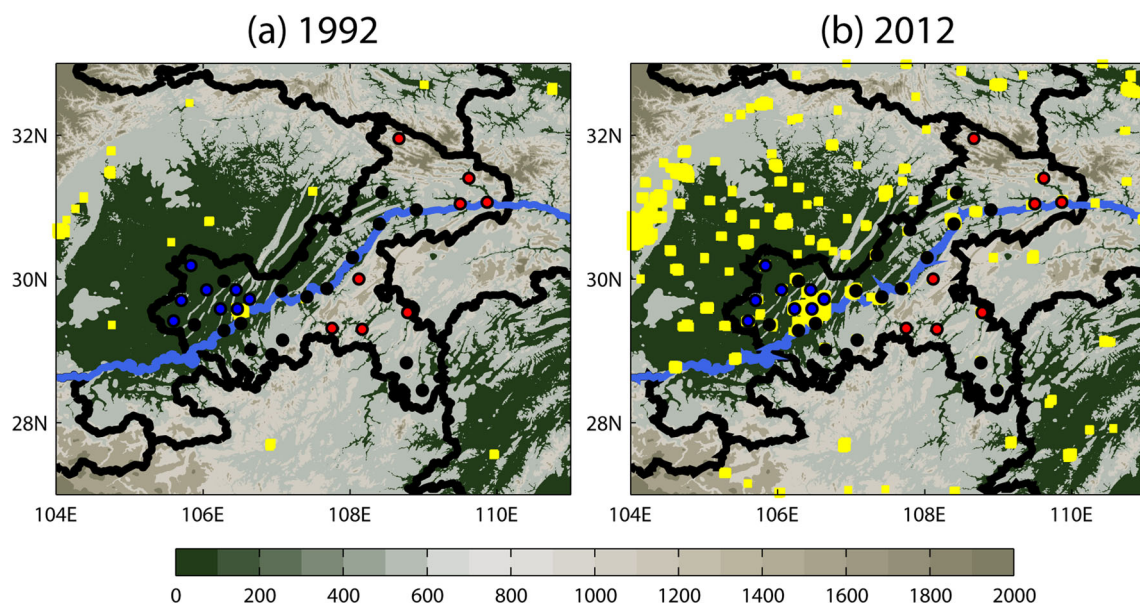


Fig. 1 The terrain altitude in the unit of meter above sea level in Chongqing with urban area in **a** 1992 and **b** 2012. The blue dots denote the basin stations, the red dots the mountain stations, while the black dots in between (i.e., the stations denoted by the black dots are neither in basin

nor on mountain). The yellow squares denote the urban area. The thick black borderline in the center of the map is the administrative boundary of Chongqing City

understanding the formation mechanism of precipitation and local climate change over complex terrain.

Using the hourly precipitation data at 34 gauge stations in Chongqing, three spatial and temporal factors of precipitation are analyzed: the precipitation amount (PA), precipitation intensity (PI) and precipitation frequency (PF), and the diurnal variation of precipitation in Chongqing is discussed. The observed data and method of analysis are briefed in Section 2. The distribution characteristics and interannual variation of precipitation in Chongqing are analyzed in Section 3. Section 4 is focused on the diurnal variation of precipitation, with its overall characteristics, propagation and interannual variation revealed. Different diurnal variation of precipitation over different terrain in Chongqing is discussed and the cause

for the difference is explained in Section 5. The dynamical environmental field in Chongqing is analyzed in Section 6. A significance test on the validity of the period of the observed data is conducted in Section 7. The study is concluded in Section 8.

2 Data and method

2.1 Data

The hourly gauge-observed precipitation data at 34 stations (Fig. 1) in Chongqing, which are provided by Chongqing Meteorological Bureau and span from 1991 to 2012, are used

Table 1 Basic information of 34 gauge stations in Chongqing

| Name | Station ID no. | Longitude (E) | Latitude (N) | Altitude (m) ASL |
|-----------|----------------|---------------|--------------|------------------|
| Chengkou | 57333 | 108° 40' | 31° 57' | 800.0 |
| Kaixian | 57338 | 108° 26' | 31° 12' | 166.4 |
| Yunyang | 57339 | 108° 54' | 30° 58' | 206.5 |
| Wuxi | 57345 | 109° 37' | 31° 24' | 339.8 |
| Fengjie | 57348 | 109° 30' | 31° 03' | 608.3 |
| Wushan | 57349 | 109° 52' | 31° 04' | 270.8 |
| Tongnan | 57409 | 105° 50' | 30° 11' | 248.1 |
| Dianjiang | 57425 | 107° 21' | 30° 20' | 418.2 |
| Liangping | 57426 | 107° 48' | 30° 41' | 459.4 |
| Wanzhou | 57432 | 108° 24' | 30° 46' | 188.8 |
| Zhongxian | 57437 | 108° 02' | 30° 18' | 232.2 |
| Shizhu | 57438 | 108° 07' | 30° 00' | 569.5 |
| Dazu | 57502 | 105° 42' | 29° 42' | 393.6 |
| Rongchang | 57505 | 105° 36' | 29° 25' | 330.0 |
| Yongchuan | 57506 | 105° 53' | 29° 22' | 319.6 |
| Wansheng | 57509 | 106° 56' | 28° 57' | 325.7 |
| Tongling | 57510 | 106° 03' | 29° 51' | 282.1 |
| Beibei | 57511 | 106° 27' | 29° 51' | 242.9 |
| Hechuan | 57512 | 106° 17' | 29° 58' | 231.1 |
| Yubei | 57513 | 106° 38' | 29° 43' | 438.0 |
| Bishan | 57514 | 106° 14' | 29° 35' | 289.2 |
| Chongqing | 57516 | 106° 28' | 29° 35' | 260.4 |
| Jiangjin | 57517 | 106° 17' | 29° 17' | 209.0 |
| Banan | 57518 | 106° 31' | 29° 23' | 205.1 |
| Nanchuan | 57519 | 107° 05' | 29° 09' | 559.5 |
| Changshou | 57520 | 107° 04' | 29° 50' | 379.0 |
| Fuling | 57522 | 107° 25' | 29° 45' | 274.1 |
| Fengdu | 57523 | 107° 41' | 29° 52' | 214.8 |
| Wulong | 57525 | 107° 45' | 29° 19' | 406.4 |
| Qianjiang | 57536 | 108° 47' | 29° 32' | 608.8 |
| Pengchui | 57537 | 108° 10' | 29° 18' | 321.5 |
| Qijiang | 57612 | 106° 39' | 29° 01' | 252.7 |
| Youyang | 57633 | 108° 46' | 28° 50' | 665.8 |
| Xiushan | 57635 | 108° 59' | 28° 27' | 363.5 |

in this study. The brief information of the stations is shown in Table 1. The grid elevation data is from USGS with a horizontal resolution of $0.00833^\circ \times 0.00833^\circ$.

The lightning data are from the Chongqing Lightning Detection Network and cover Chongqing City. The data are put into the grid of 20×20 km for comparative analysis.

The ECMWF ERA-Interim Reanalysis Dataset (ERA-Interim) is used for analyses of the environment circulation field and humidity field with a temporal resolution of 6 h and a horizontal resolution of $0.75^\circ \times 0.75^\circ$ (Dee et al. 2011).

2.2 Method

Firstly, the observations have been homogenized. Although some observation stations have been relocated to nearby sites, which are very close to original locations, the impact on the observed precipitation is negligible. No correction is made for the observations and missing values are ignored. The gaps existed only for a short time, thus the statistical results obtained by directly processing the data are not affected. Using the hourly precipitation data, the

spatial and temporal characteristics of the PA, PI and PF are calculated and analyzed. For a study period, the PA is the total precipitation amount divided by the total hours, the PI the precipitation intensity that is the total precipitation amount divided by the total precipitating hours, and the PF the precipitation frequency that is the total precipitating hours divided by the total hours. These formulae are shown as follows:

$$PA = \frac{\sum_{t=1}^n P_t}{n} \quad (1)$$

$$PI = \frac{\sum_{t=1}^n P_t}{\sum_{t=1}^n i} \quad (\text{when } P_t \geq 0.1 \text{ mm}, i = 1; \text{ otherwise, } i = 0) \quad (2)$$

$$PF = \frac{\sum_{t=1}^n i}{n} \quad (\text{when } P_t \geq 0.1 \text{ mm}, i = 1; \text{ otherwise, } i = 0). \quad (3)$$

The harmonic analysis is one of the methods used to calculate the diurnal variation of precipitation. It extracts the harmonic waves with different amplitudes and phases from

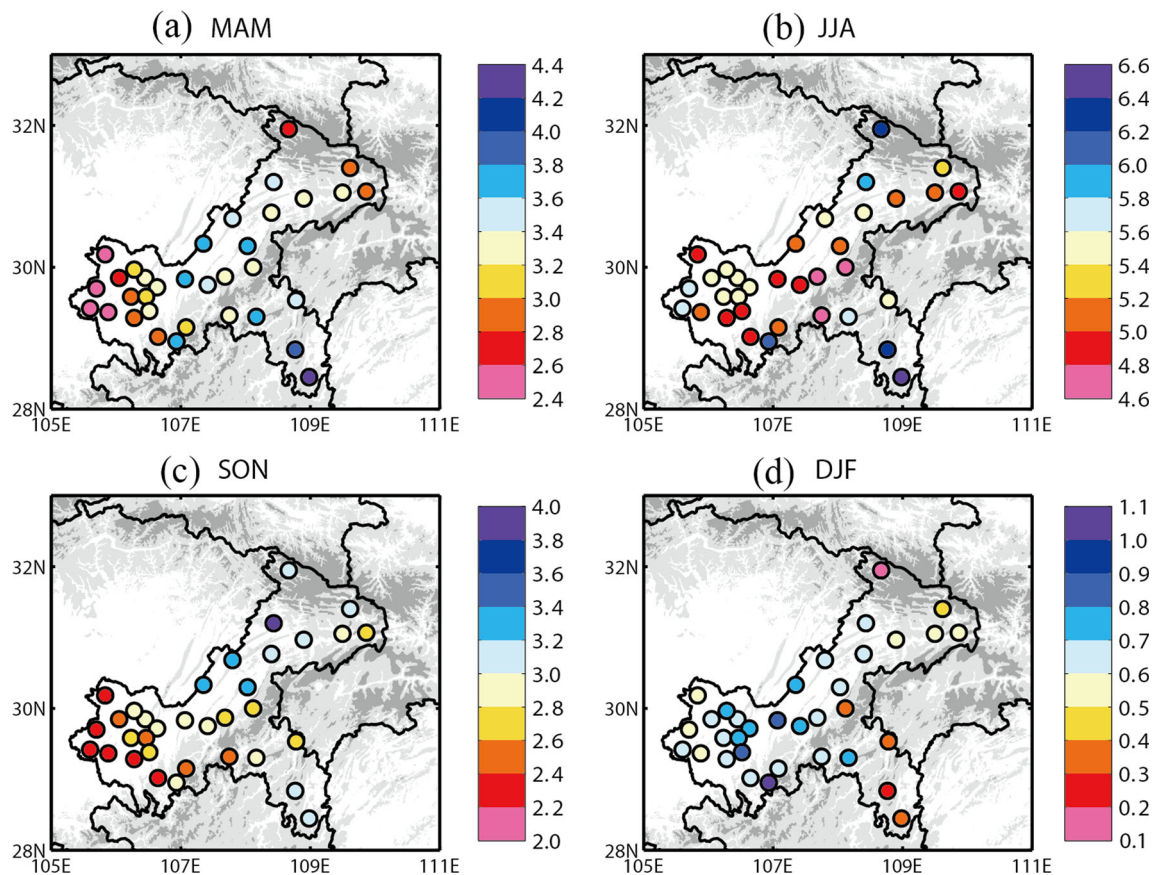


Fig. 2 The spatial distribution of seasonally averaged precipitation at 34 stations in four seasons in Chongqing in the unit of mm/day. Lightly shaded are the areas higher than 600 m above sea level, while the darkly shaded areas higher than 1200 m above sea level

the irregular vibration curve (Wallace 1975). According to the Fourier transformation theory, if a time function $f(t)$ with a period of T meets certain conditions, it can be expressed as the sum of a series of harmonic waves, which is

$$f(t) = C_0 + \sum_{k=1}^{\infty} C_k \sin(\omega_k t + \phi_k) \tag{4}$$

where C_0 is the average of $f(t)$, C_k the amplitude of a harmonic wave, $\omega_k = \frac{2\pi k}{T}$ the frequency of the harmonic wave, and ϕ_k the initial phase of the harmonic wave. For discrete time series, the maximum number of harmonic waves is $N/2$ (e.g., if there are 8 values a day, the maximum number of harmonic waves is 4).

Using the harmonic analysis method and referring to previous research (Rouault et al. 2013), the standardized amplitude $\left(\frac{C_k}{2C_0}\right)$ as well as the portion of variance $\left(\frac{C_k^2}{2\sigma^2}\right)$, where σ is the standard deviation of the precipitation factors) are calculated to reveal the relative importance of diurnal variation.

The diurnal percentage index (DPI) of precipitation is used to measure the magnitude of diurnal variation of precipitation relative to the average state of the local precipitation, in order

to compare different stations with different mean precipitations. The formula is as follows:

$$DPI = \frac{\sum_{t=1}^{24} |r_t - \bar{r}|}{r_d} \tag{5}$$

where r_t is the hourly precipitation, \bar{r} the hourly averaged precipitation, and r_d the daily-averaged precipitation (Bao et al. 2011).

3 The climatic characteristics of precipitation in Chongqing

Located at the edge of the Sichuan Basin, the southwestern Chongqing is largely inside the Sichuan Basin and of low elevation. In the middle a crescent mountain higher than 1200 m above sea level gradually raises eastward, cutting into the middle Chongqing from the southwest to the northeast (Fig. 1). Figure 2 shows the distribution of the seasonally averaged PA in four seasons from 1991 to

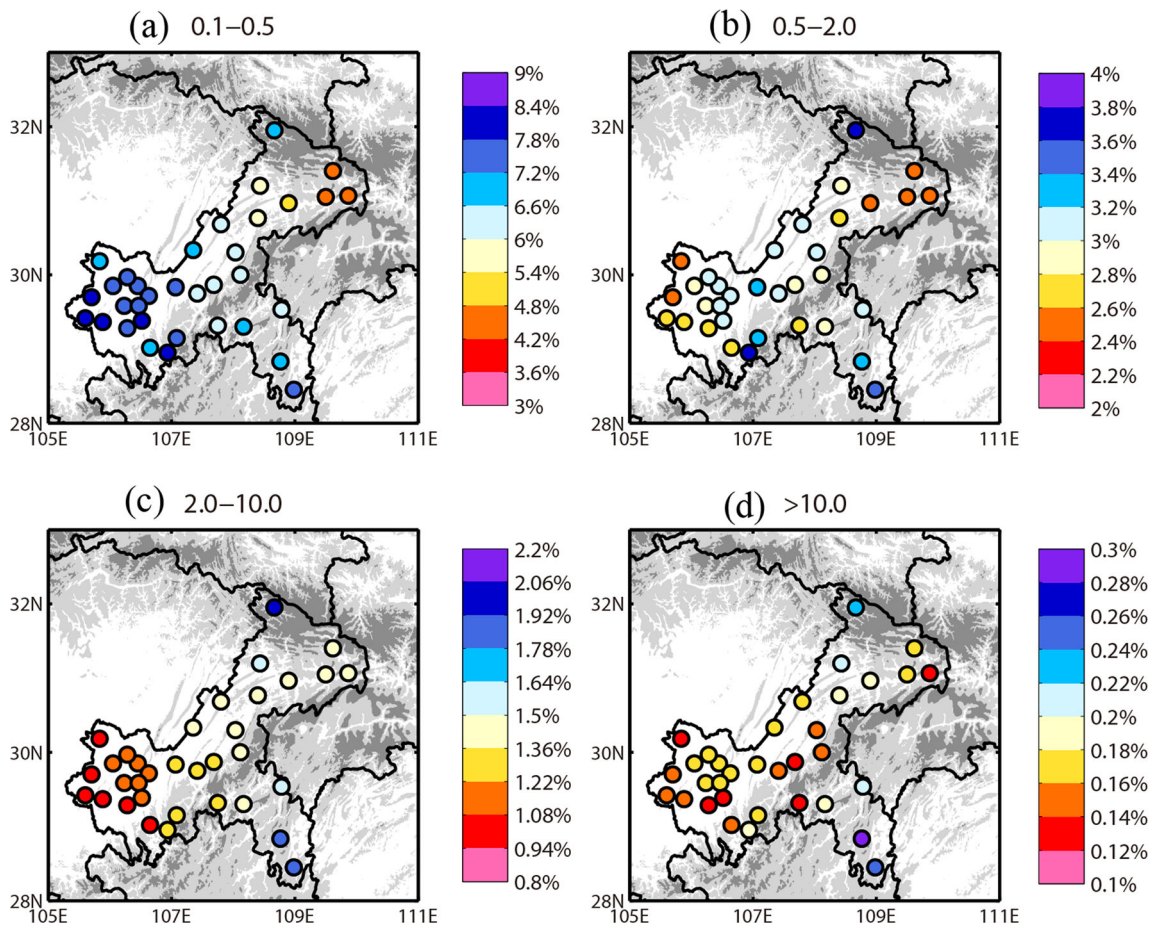


Fig. 3 The spatial distribution of the PF in different levels of precipitation intensity in mm/h. Lightly shaded are the areas higher than 600 m above sea level, while the darkly shaded areas higher than 1200 m above sea level

2012 at 34 stations in Chongqing. Affected by the monsoon and topography, Chongqing’s rainfall is abundant. Summer is the season with the most rainfall, followed by spring and autumn. In terms of season, the spatial distribution of precipitation also displays apparent inhomogeneity. In spring and autumn, the precipitation in the southwestern Chongqing was generally lower than in the east and middle Chongqing. However, in summer, except in the southeastern area, the distribution of precipitation was generally contrary to that in spring. The PA at most stations in the basin was higher than on the middle and northeastern highlands. The distribution of precipitation in winter was in correspondence with the terrain altitude, and the precipitation in the basin was higher than on the highlands.

The precipitation intensity is classified into four levels: 0.1 mm/h–0.5 mm/h, 0.5 mm/h–2.0 mm/h, 2.0 mm/h–10.0 mm/h, and > 10.0 mm/h. The PF is calculated for each station (Fig. 3). The PF with the precipitation intensity being 0.1 mm/h–0.5 mm/h at each station was evidently higher than with the other levels. The PF was lower when the precipitation was stronger. For the first level, it can be found that the probability of precipitation at the basin stations was significantly higher than at the middle and northeastern highlands stations, while the northeast stations had the lowest probability of precipitation. With the precipitation intensity increasing to 2.0 mm/h–10.0 mm/h, the PF at the basin stations decreased and was less than at the other stations, indicating the terrain had a significant impact on the characteristics of precipitation. When the precipitation intensity was over 10.0 mm/h, the PF at all the 34 stations in Chongqing was very low, but the high-intensity precipitation in this level was more likely to occur at the stations in the southeast and northeast area than at the other stations.

4 Diurnal variation of precipitation

Figure 4 is the diurnal cycle of the mean PA, PI, and PF in four seasons in Chongqing. It can be seen that the PA had a clear peak in the early morning, which appeared around 0300 LST (1900 UTC) in spring and around 0800 LST (0000 UTC) in autumn. The peak value was larger than 0.25 mm/h in spring but less than 0.2 mm/h in autumn. In summer, the PA had a bimodal structure with a peak larger than 0.3 mm/h at 0800 LST (0000 UTC) and a peak about 0.2 mm/h at 1600 LST (0800 UTC). The diurnal variation of the PF was similar to that of the PA, with two peaks in summer and a single peak in the other seasons. However, it should be noted that from 0000 LST to 1200 LST, the PF in spring and autumn was larger than in summer. Although the PA during this period in summer was not significantly larger than in spring and autumn, the PI in summer was significantly higher than in spring

and autumn due to the decrease of the PF. Compared with the PA and PF, the diurnal variation of the PI was not very evident, which may indicate the diurnal variation of the PA was associated with the diurnal variation of the PF. In general, the diurnal variation of the PA and PF in Chongqing showed that the nighttime rain was evident in this area (Bao et al. 2011; Tang et al. 2011; Chen et al. 2012a, b; Wang et al. 2011; Xue et al. 2012; Qian et al. 2015).

The peak time of the precipitation factors also reflected the main characteristics of diurnal variation of precipitation. Figure 5 shows the spatial distribution of the time at which the seasonally-averaged precipitation amount peak (PPA), precipitation intensity peak (PPI), and precipitation frequency peak (PPF) appeared. In terms of the spatial distribution, the PPA time at the southwest basin stations largely appeared in the early morning in spring, autumn and winter and was delayed to about 0800 LST (0000 UTC) at some stations in summer. In summer the PPA at three stations appeared around 1600 LST (0800 UTC), indicating the precipitation amount in the afternoon was larger than in the morning and the PPA in the afternoon was the main peak. In terms of the overall trend, the peak time at

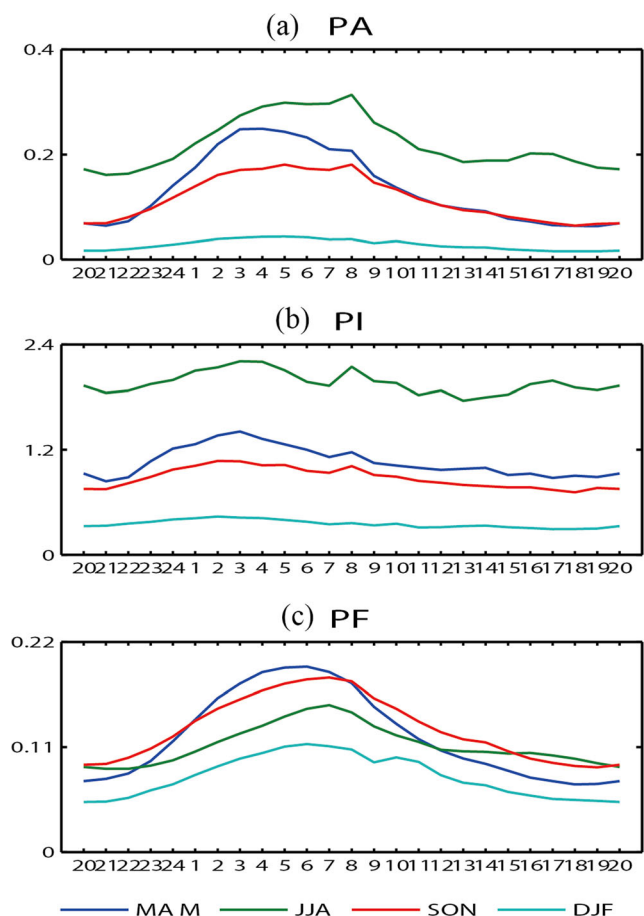
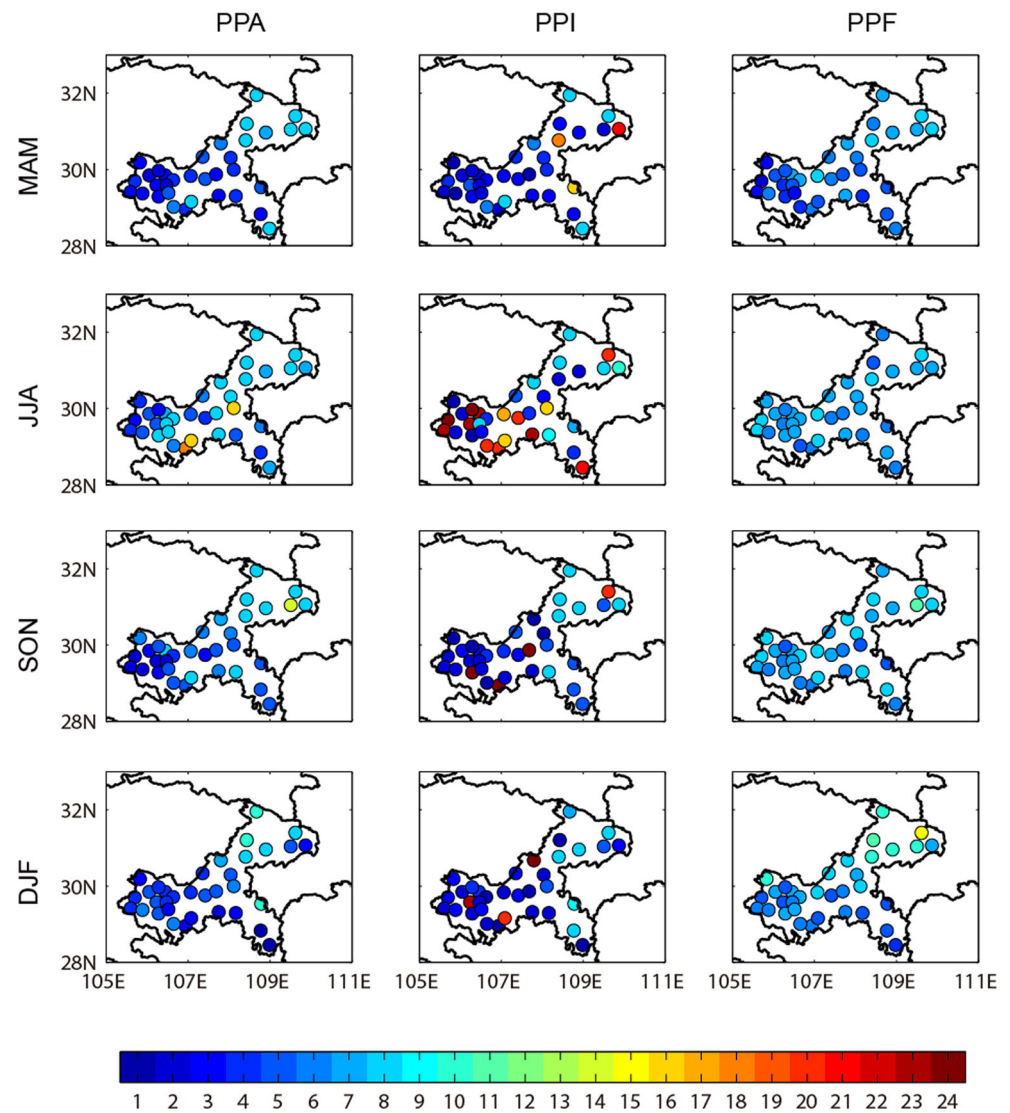


Fig. 4 The diurnal variation of the precipitation factors (PA, PI, and PF) averaged over all the stations. The PA and PI are in mm/h

Fig. 5 The spatial distribution of peak time of the seasonally averaged precipitation factors (PA, PI, and PF) in Chongqing



the stations in the northeastern Chongqing in each season significantly lagged behind those in the southwest area with the lag time about 6 h. The PPI time was several hours ahead of the PPA time throughout the year in the basin and middle Chongqing, especially in summer. The PPI time at the stations in the basin was around 0000 LST (1600 UTC), and at several stations was around 1600 LST (0800 UTC) in the afternoon in summer. The PPI time in spring and autumn was the same as the PPA time at most stations in the northeast and southeastern Chongqing. In summer, some peaks appeared in the early morning. Thus overall the diurnal variation of the PI was not in a regular pattern, which supports the previous description. The spatial distribution of the PPF time was similar to that of the PPA time, but in the basin it evidently lagged behind the PPA and PPI time in the same season.

Figure 6 shows the results of the harmonic analysis for the diurnal variation of the PA at the 34 stations in Chongqing in

different seasons. The value of the harmonic analysis reflects the intensity of diurnal variation of the PA. The larger the value is, the stronger the intensity of diurnal variation is (Rouault et al. 2013; Roy and Balling 2014). Similar to the previous results, the value of the harmonic analysis in summer was smaller than in the other seasons, indicating the intensity of diurnal variation in summer was less than in the other seasons. Moreover, the intensity of diurnal variation was stronger in spring and autumn than in winter. In terms of the spatial distribution in spring and autumn, the diurnal variation of the PA was strongest in the basin lower than 600 m above sea level. When the elevation is about 600–1200 m in the middle and southeastern Chongqing, the values of the harmonic analysis decrease. When the elevation reaches 1200 m in the northeastern Chongqing, the values of the harmonic analysis are least, indicating the diurnal variation of the PA was weakest there. This reveals the values are decreasing with increasing elevation. Although the difference between

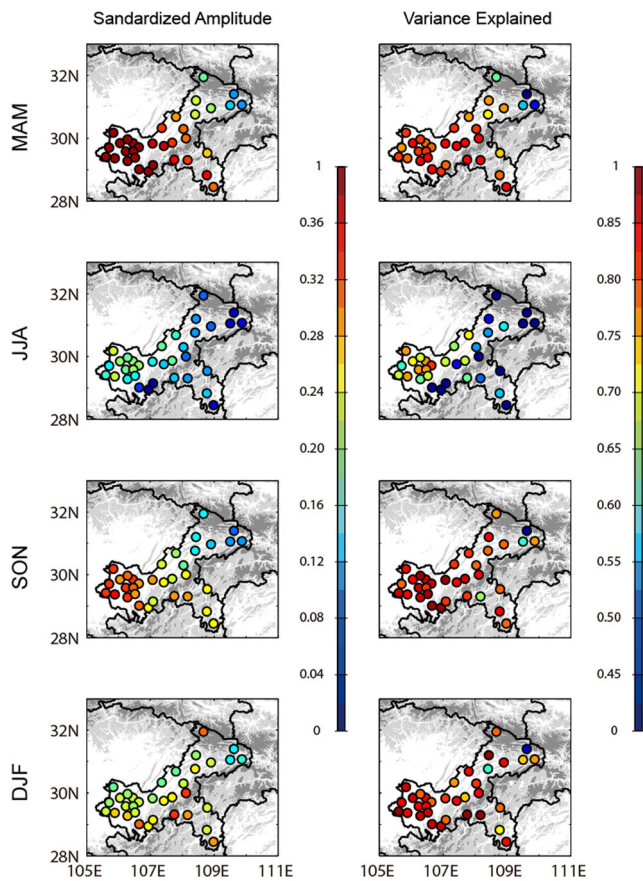


Fig. 6 The harmonic analysis of diurnal variation of the PA. The first harmonic wave is used. The closer the value is to 1, the stronger the intensity of diurnal variation is. Lightly shaded are the areas higher than 600 m above sea level, while the darkly shaded areas higher than 1200 m above sea level

adjacent stations was small in winter and summer, when comparing the stations in the basin to those on the high-altitude mountain, it still can be seen that the intensity of diurnal variation decreases with increasing elevation. The results of the harmonic analysis for the diurnal variation of the PF are similar to those of the PA (not shown here). Compared with the results of the PA and PF, the diurnal variation of the PI was evidently smaller, indicating the intensity of diurnal variation of the PI was weaker than those of the PA and PF. In spring and autumn, the intensity of diurnal variation of the PI decreased with increasing elevation, while there was no clear trend in summer and winter (not shown here).

Figure 7 shows the DPI distribution at 34 stations in Chongqing. The larger the value is, the stronger the fluctuation of diurnal variation is. According to Eq. (5), since at each station the impact of the precipitation amount on the DPI is excluded, the intensity of diurnal variation at different stations can be compared objectively. In spring, the DPI reached 60 to 80% in the basin while was about 40 to 50% at the middle and southeastern stations, and the DPI at the northeast stations was less than 30%. Therefore the DPI was different on different

terrains in spring, and it was stronger in the basin and weaker in the mountainous area. The characteristics of diurnal variation in autumn were similar to those in spring, but the DPI at the stations in the basin was about 50%, indicating the intensity of diurnal variation of precipitation was weaker than in spring. The DPI was less than 30% in summer and less than 45% in winter, suggesting the intensity of diurnal variation of precipitation in summer and winter was weaker than in spring and autumn, and the difference in the distribution of the DPI on different terrains was almost negligible in summer and winter.

The interannual variation is an important characteristic of precipitation (Klingaman et al. 2013; Siderius et al. 2014). Due to short temporal length of data, previous researches rarely looked into the interannual variation of precipitation. In this study, the interannual variation of diurnal variation of precipitation based on the amplitude of diurnal variation of the precipitation factors is investigated to reveal the magnitude of the intensity of diurnal variation of precipitation. Figure 8 shows the interannual variation of the seasonally averaged amplitudes of diurnal variation of the PA, PI, and PF. The interannual variability of the PA, PI, and PF in each season was evident, and the amplitude of the precipitation factors was significantly different in different season. In spring, the amplitude of the PA was between 0.1–0.3 mm/h, the amplitude of the PF between 9% and 18%, and the amplitude of the PI less than 1.4 mm/h except in 1998, while the amplitude of the PI was larger than 0.8 mm/h with the mean amplitude about 1.5 mm/h in summer, which was higher than in the other seasons. However, the amplitude of the PF was low in summer and around 7%. In autumn, the amplitude of the PI was about 0.5 mm/h, lower than in spring and summer, while the amplitude of PF was higher than in summer. Although the amplitudes of the PA and PI in winter were lower than in the other seasons, the amplitude of the PF was close to that in summer. For the PF, the amplitudes in spring and autumn were significantly larger than in summer, especially much larger in spring. On the one hand, this indicates the diurnal variation of the PI was larger in summer, probably due to the larger amount and shorter duration of strong precipitation. On the other hand, compared to summer, weaker precipitation was more likely to happen in spring and autumn. Thus, the characteristics of precipitation in summer were very different from in spring and autumn.

5 Comparison of diurnal variation of precipitation between in the basin and in the mountainous area

Topography is one of the geographical conditions that can affect precipitation through dynamics, water vapor, and other factors (Tucker 1993; Chen et al. 2009; He and

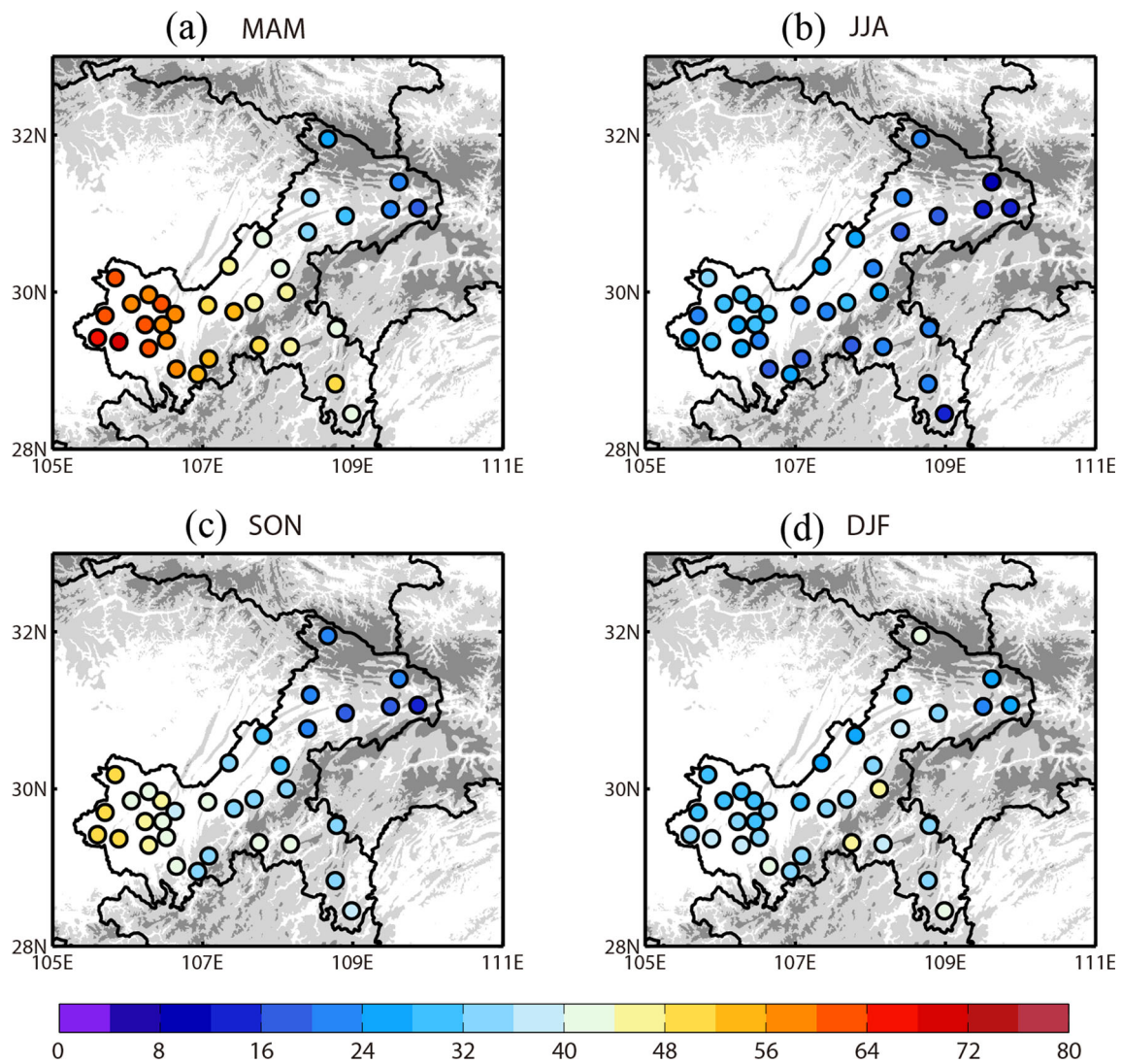


Fig. 7 The spatial distribution of the DPI (Diurnal Precipitation Index) in percentage, which measures the intensity of diurnal variation of precipitation. The larger the value is, the stronger the fluctuation of

precipitation is. Lightly shaded are the areas higher than 600 m above sea level, while the darkly shaded areas higher than 1200 m above sea level

Zhang 2010; Zhao et al. 2012; Yu et al. 2014a, b; Yuan et al. 2014). Chongqing known as “mountain city” has special geographical conditions with relatively flat terrain in the Sichuan Basin and mountains along the edge of the basin, and is rich in water resource and humid all year around. Due to complex terrain and adequate precipitation, this study on the diurnal variation of precipitation in this area could have good representativeness. In order to further study the effect of the topographic variability on the diurnal variation of precipitation, according to their geographical locations, eight stations in the basin (Station ID Nos. 57409, 57502, 57505, 57510, 57511, 57513, 57516, and 57514) and eight stations in the mountainous area (Station ID Nos. 57333, 57345, 57348, 57349, 57438, 57525, 57536, and 57537) are selected to represent the respective terrains. The effects of terrain on the type and diurnal

variation of precipitation are investigated by classifying the precipitation intensity (Landin and Bosart 1989; Yuan et al. 2010; Wang et al. 2015).

Figure 9 shows the diurnal variation of the precipitation frequency (in percentage) for different intensity (0.1–0.5 mm/h, 0.5–2.0 mm/h, 2.0–10.0 mm/h, > 10.0 mm/h) of precipitation. First, with the increasing precipitation intensity, the precipitation frequency decreased continuously but still played an important role in the diurnal variation of precipitation due to the high precipitation intensity. Second, by comparing the two curves in the same level of the precipitation intensity, the amplitude of the curve in the basin was always larger than in the mountainous area in each level, indicating the intensity of diurnal variation of precipitation in the basin was larger than in the mountainous area. Also, in the level of 0.1–0.5 mm/h, the

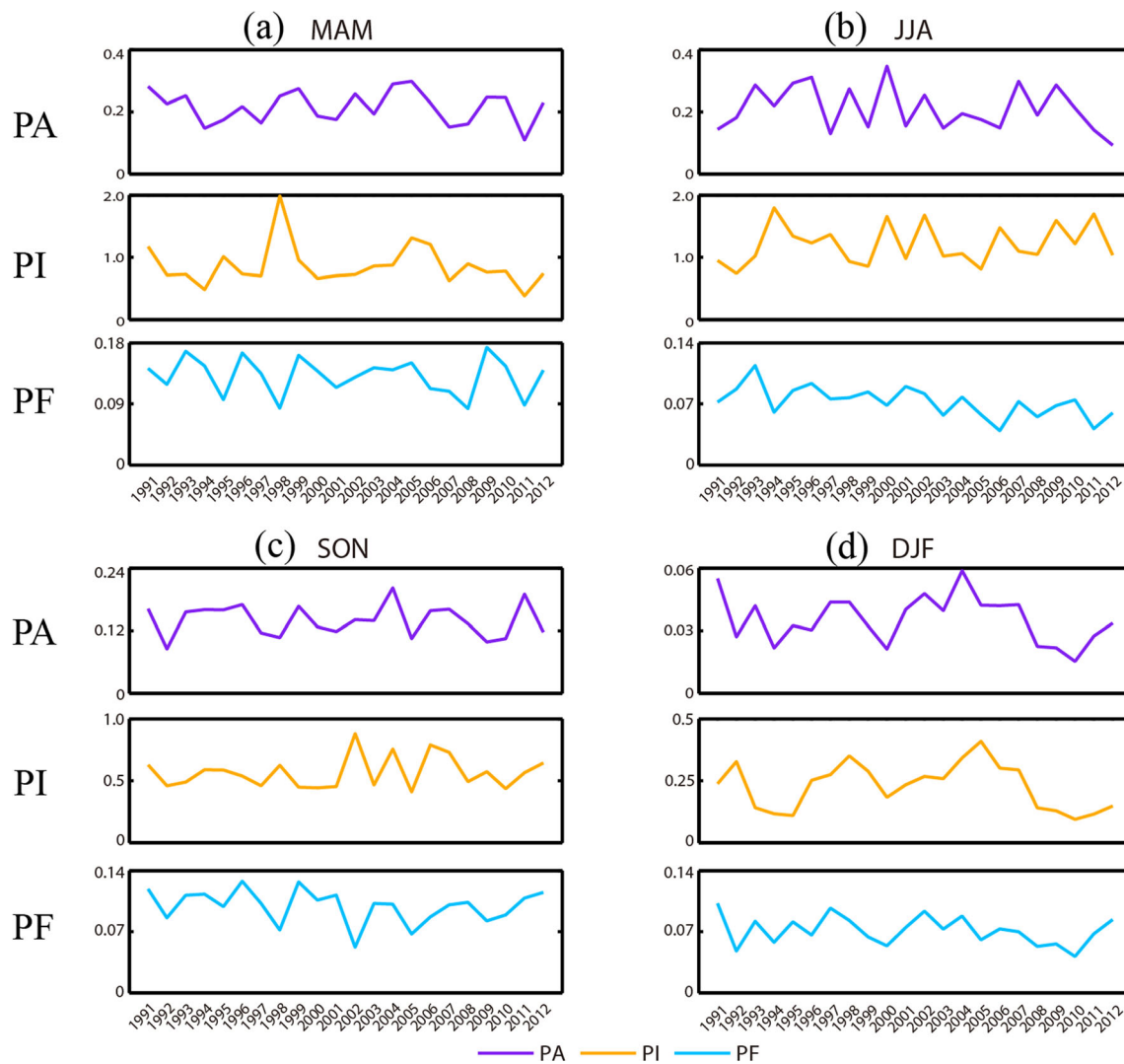


Fig. 8 The interannual variation of the seasonally averaged amplitude of diurnal variation of the PA/PI/PF. The abscissa denotes the year, while the ordinate the amplitude of the PA/PI/PF. The amplitudes of the PA and PI are in mm/h

precipitation peak was at about 0700 LST (2300 UTC) for the two types of terrain. In summer, a second peak appeared in the evening around 1900 LST (1100 UTC) in the mountainous area. In the level of 0.5–2.0 mm/h, the annual peak in the basin was at 0400 LST (2000 UTC), while the peak in the mountainous area lagged behind by about 3 h, and the intensity of diurnal variation was weaker than in the basin. In summer, there were evident peaks in the afternoon in the mountainous area, which were slightly stronger than the peak in the morning. The characteristic of diurnal variation showed a variation in M-shape, which was in strong contrast with in the basin. Although the number of precipitation days in the first two levels in the basin was significantly more than in the mountainous area, the number of precipitation days in the mountainous area was more than in the basin in the level of 2.0–10.0 mm/h. The peak time in the basin was at 0300 LST (1900 UTC) for the

annual results and at 0500 LST (2100 UTC) in summer, while in the mountainous area it lagged behind by 2–4 h and had a peak in the afternoon in summer. For the level of intense precipitation over 10.0 mm/h, the days of precipitation in the two areas were few, while there was an evident bimodal pattern in the mountainous area. The classified diurnal variation of the PA was similar to that of the PF, but that of the PI was evidently different (not shown here). The characteristics of diurnal variation of precipitation were similar in different level of precipitation intensity and on different terrain, indicating the trend of diurnal variation of the PA was largely affected by the PF.

In terms of the level of precipitation intensity, the difference in precipitation between in the mountainous area and in the basin was mainly in the levels of over 0.5 mm/h. With heavy rainfall, especially when the strong convective weather appears, lightning is often associated. Therefore,

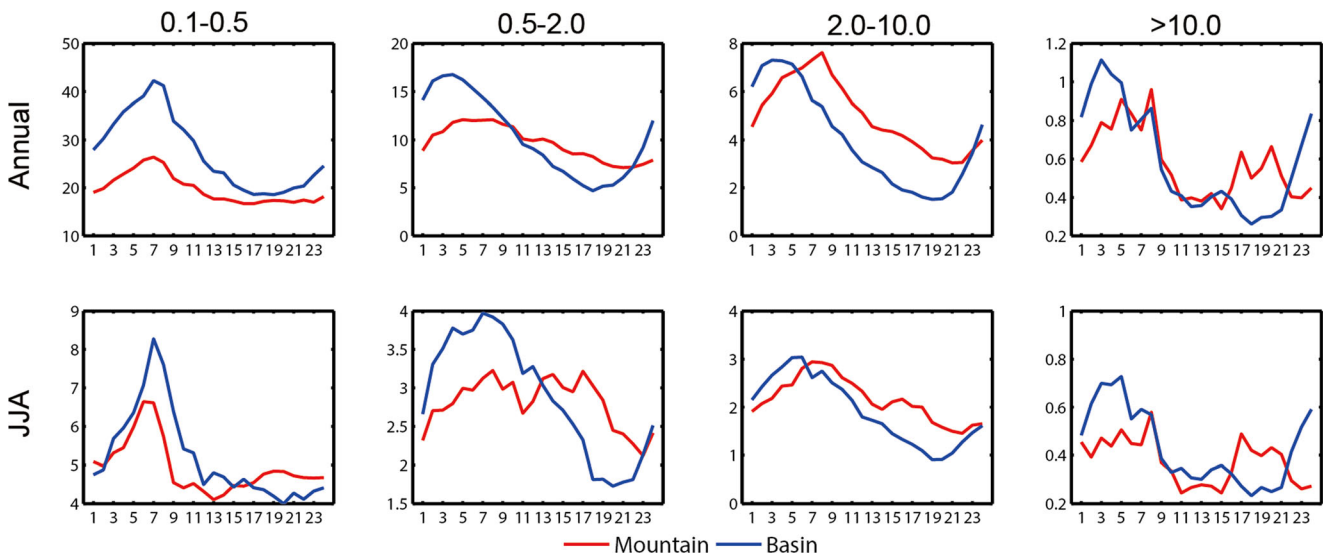


Fig. 9 The diurnal variation of the PF (in percentage) in different levels of precipitation intensity in mm/h in the basin and mountainous area. The four levels of precipitation intensity are 0.1–0.5 mm/h, 0.5–2.0 mm/h,

2.0–10.0 mm/h, and larger than 10.0 mm/h. In the first row are the annually averaged results, while in the second row the results averaged over the summer

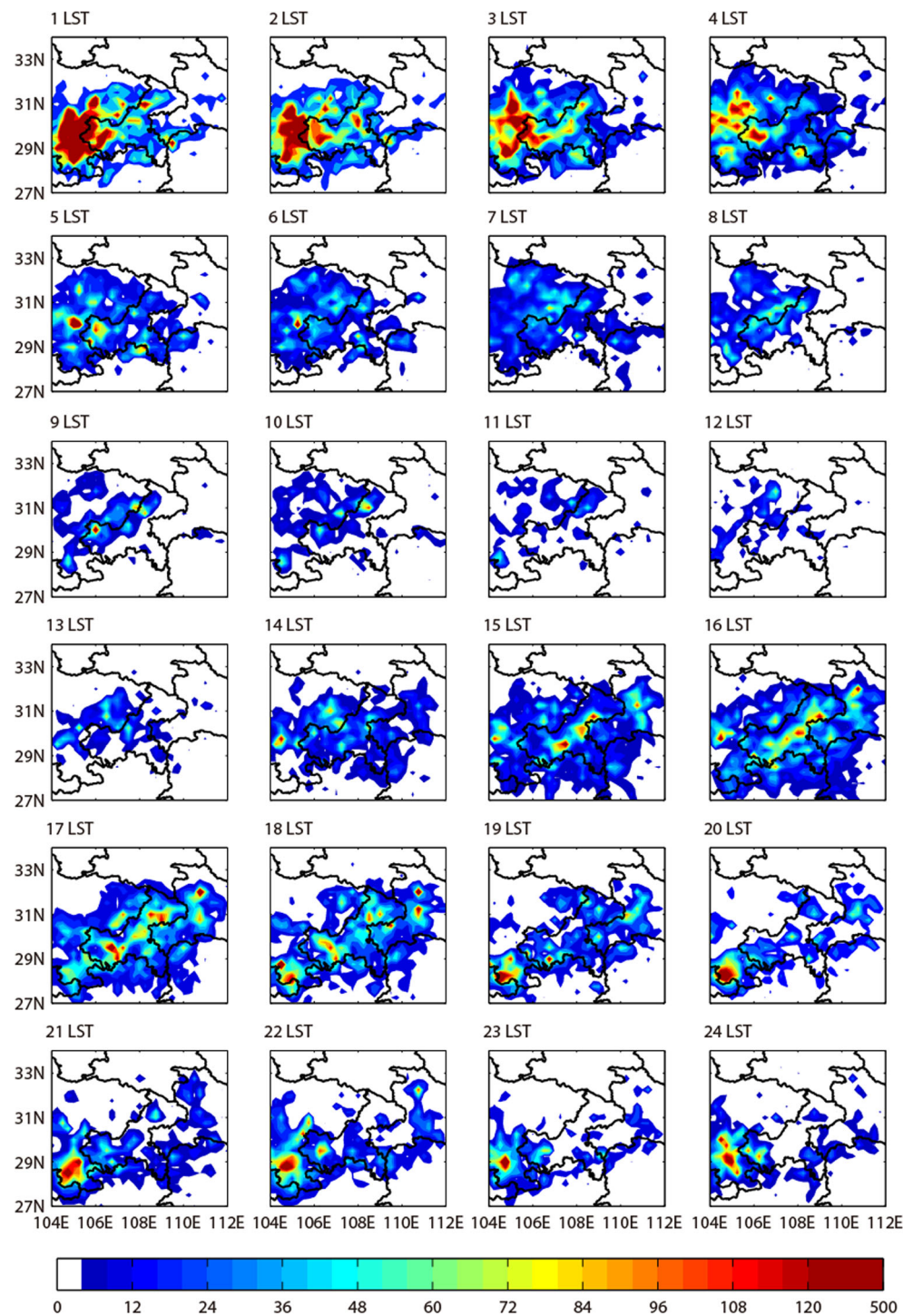
analyzing the diurnal variation of lightning data is helpful in the study on the diurnal variation of precipitation. Figure 10 shows the spatial distribution of diurnal variation of lightning in summer over Chongqing from 2008 to 2014. Seen in Fig. 10, there were two periods of frequent lightning flash in Chongqing in the night and afternoon. The lightning after 2100 LST (1300 UTC) reached the strongest from 0100 LST (1700 UTC) to 0200 LST (1800 UTC) the next day in the southwest Chongqing and inside the Sichuan Basin, and then spread to the eastern mountainous area of Chongqing. After all the areas were covered at 0400 LST (2000 UTC), the extent began to shrink. The strength reduced and reached the weakest in the morning at around 0900 LST (0100 UTC) at the edge of the basin. The lightning thunderstorm largely originated in the basin in the night, spreading to the edge, and then disappeared in the afternoon the next day. Another period of frequent lightning started around 1300 LST (0500 UTC), with the lightning reaching its peak around 1600 BT (0800 UTC) to 1700 BT (0900 UTC) and then dissipating after 1800 LST (1000 UTC). Unlike the nocturnal lightning, the lightning reached the strongest in the afternoon largely in the eastern and middle Chongqing. The period of development was shorter and the extent was smaller, and the influence area did not spread to the basin. This is in consistency with the diurnal precipitation that had an evident second peak in the afternoon in the mountainous area while had no one in the basin. The phenomenon was more evident in the levels of higher precipitation intensity. The greatest difference in lightning distribution between in spring (not shown here) and in summer was that in spring there were almost no lightning processes in the afternoon with just sporadic lightning events in the mountainous area.

6 Analysis of environmental field in Chongqing

Analyzing the characteristics of environmental field in Chongqing at different times of a day is helpful in understanding the formation mechanism of diurnal variation of precipitation and its areal difference. In this study, the variations of the vorticity field and vertical movement are examined to further understand the characteristics of diurnal variation of precipitation.

Figure 11 shows the vertical movement and the vorticity field on 850 hPa at four times of a day in different seasons in Chongqing. The shaded colors denote the vertical movement and the contours of the vorticity field at the interval of $1.5 \times 10^{-6} \text{ s}^{-1}$ with purple for positive and green for negative. Due to the large time interval, the seasonal difference in the vorticity and vertical movement was not evident. Thus, we take the summer as an example. Most of the areas in Chongqing were under the control of the updraft at 0200 LST (1800 UTC), and the updraft in the southwestern area was strongest with strong positive vorticity center, providing sufficient dynamical conditions for the formation of precipitation. At 0800 LST (0000 UTC), the southwestern Chongqing in the Sichuan Basin was still under the control of the updraft and at the center of positive vorticity. Except the southeast area, the other areas were under the control of the downdraft, explaining why the precipitation in the basin from late night to early morning was evidently stronger than in the mountainous area. At 1400 LST (0600 UTC) in the afternoon, Chongqing was controlled by the updraft induced by radiation, especially in the mountainous area with the maximum vertical speed, providing sufficient dynamical conditions for the formation of the second peak of precipitation in the afternoon in the mountain area,

Fig. 10 The spatial distribution of diurnal variation of summer lightning in Chongqing during the period of 2008–2014. The unit is measured in number of occurrence per year in a grid of $0.25^\circ \times 0.25^\circ$



while the vorticity was weaker than in the night and early morning. Due to the radiation effect that is significantly different after the sunset and the location of the mountainous area in the eastern Chongqing, the circulation characteristics of the mountain-valley breeze are common. At 2000 LST (1200 UTC) in the evening, there was the updraft along the edge of the mountainous area with positive vorticity center located at the northeastern edge of Chongqing.

In terms of the vertical movement and vorticity field, from late night to early morning, the dynamical conditions in the basin were more favorable for precipitation than in the mountainous area. In the afternoon, the updraft induced by solar radiation was strong and kept in the mountainous area until 2000 LST (1200 UTC) in the night, which were favorable for the second peak of precipitation in the mountainous area in the afternoon.

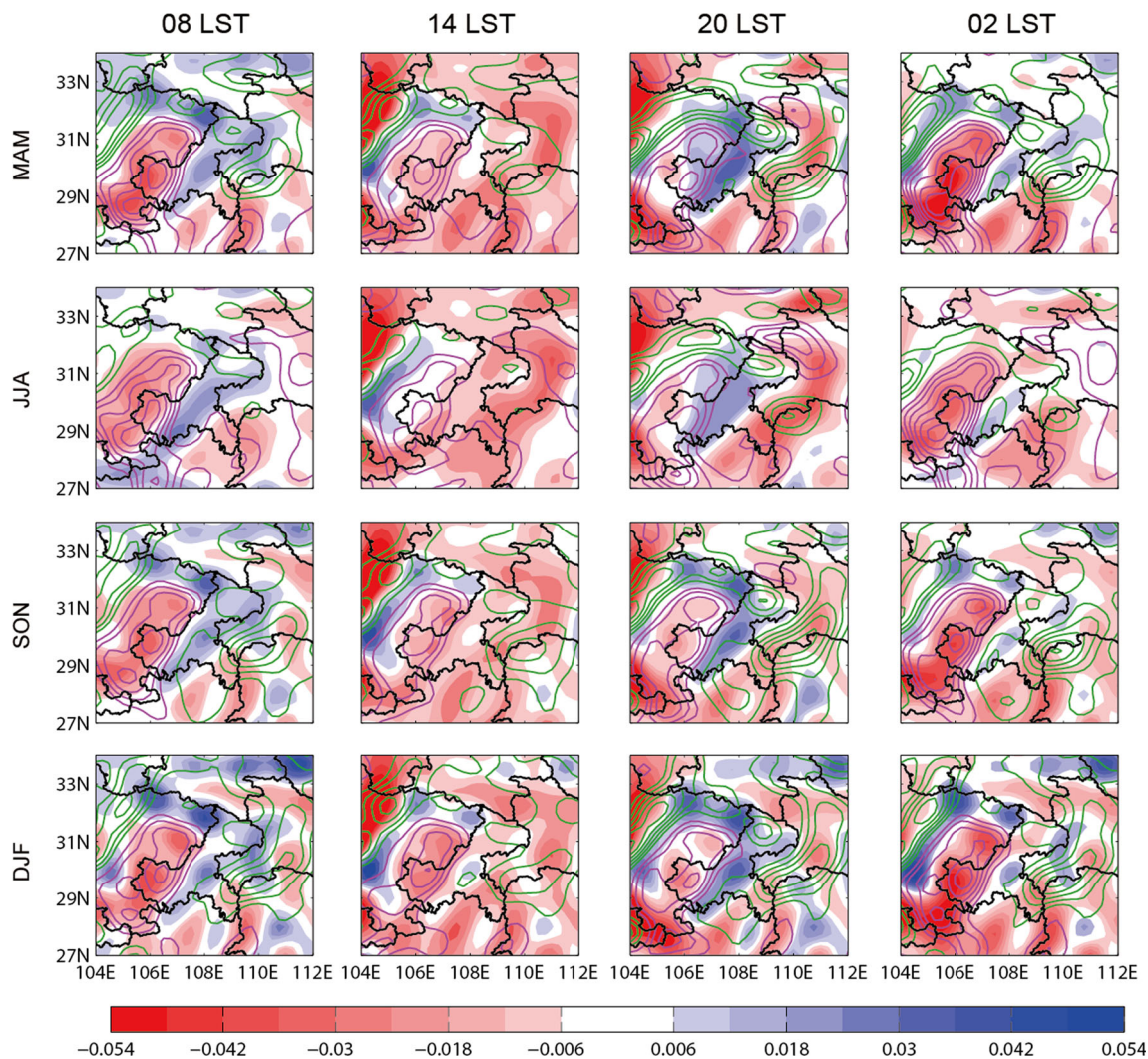


Fig. 11 The diurnal variation of the vertical movement and vorticity field on 850 hPa in four seasons in Chongqing. The vertical velocity is in pa/s

7 Significance test

To check the validity of the period of the observed data with significance test, the F test (joint hypotheses test) is applied to the trend analysis. Figure 12 shows the linear trends of the seasonally averaged precipitation at 34 stations in Chongqing. In spring, there are negative trends in most of the basin and northeastern Chongqing and positive trends in the southeastern Chongqing. In summer, the precipitation has negative trends in most of the middle and southeastern Chongqing and positive trends are dominant in the basin and northeastern Chongqing. The positive trends in autumn are in the northernmost and southernmost Chongqing, while the negative trends are dominant in the rest of Chongqing. In winter, only the precipitation at the stations in the southeastern Chongqing has positive trends. Moreover, it can be seen in the figures that at most of the stations the significance level of 0.1 has not been passed,

suggesting the trend analysis is not significantly associated with the period of the observed precipitation data.

8 Conclusions and discussion

With the analysis on the hourly precipitation data in Chongqing from 1991 to 2012, the understanding of the characteristics of precipitation in Chongqing is furthered. Focused on the diurnal variation of precipitation, its mean characteristics, interannual variations and areal differences are investigated, and the reasons for the areal differences are explained. The main conclusions are as follows:

- (1) The PA in Chongqing in spring and autumn was larger in the east and less in the west. The summer PA was dominant throughout the year, and the precipitation in the basin was more than in the eastern and middle

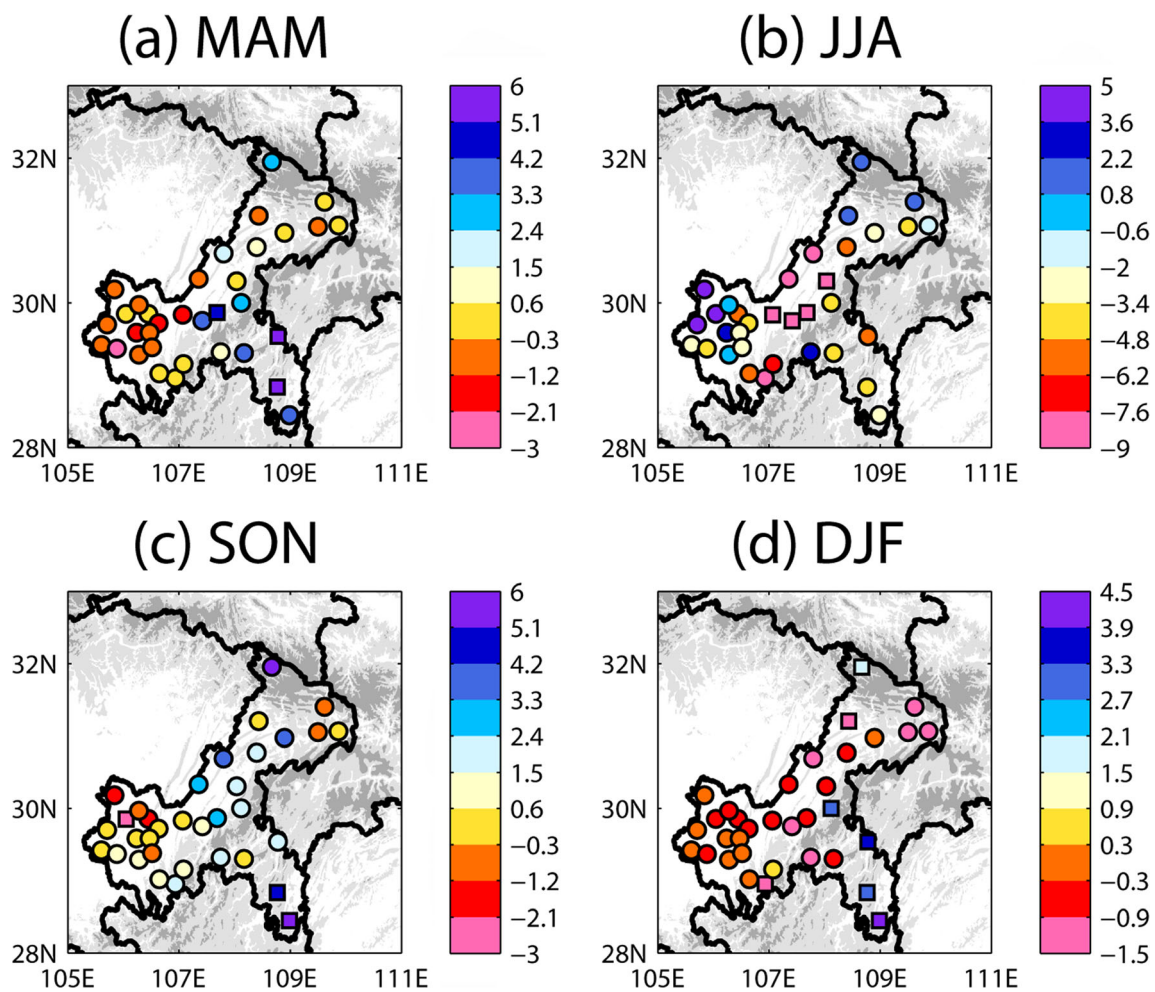


Fig. 12 Linear trends of the seasonally-averaged precipitation in mm/year at 34 stations in Chongqing. The squares denote the stations where the significance level of 0.1 has been passed, while at the other stations denoted by the dots it has not been passed

mountainous area, which was very different from in spring and autumn. The winter precipitation was least and the distribution characteristics were similar to those in summer.

- (2) The nocturnal precipitation in Chongqing was evident, and the peak times of the precipitation factors were generally from the midnight to the early morning. The intensity of diurnal variation of the PF was evidently stronger than that of the PI, which determined the main characteristics of diurnal variation of the PA.
- (3) The peak times of the precipitation factors at the mountainous stations in the northeastern Chongqing lagged behind those at the basin stations in the southwest. The phenomenon was more evident for the PF, compared to the PI.
- (4) The amplitudes of the PI and PF had significant seasonal distinctions. The amplitude of the PI in summer was evidently higher than in the other seasons, while that of the PF was higher in spring and autumn than in summer, especially much higher in spring. There were significant

interannual variations in the amplitudes of the precipitation factors in spring and summer, while their trends of variation were contrary to each other in terms of season.

- (5) Terrain was one of the factors closely related to the diurnal variation of precipitation. The higher the altitude was, the weaker the intensity of diurnal variation of precipitation was. Based on the diurnal variation in terms of the level of precipitation intensity and distribution of lightning, the enhancement of precipitation in the afternoon in the mountainous area was due to the short-time heavy precipitation caused by the convection in the afternoon.

The study could be helpful in further understanding the precipitation characteristics in Chongqing and in researches on precipitation over complex terrain in the southwest China. However, due to the limited data length, inhomogeneous spatial distribution of the stations, and scarce records of precipitation in sparsely populated areas, this study may be further improved in future works.

Acknowledgements The authors are thankful to Chongqing Meteorological Bureau for providing the observed precipitation data.

Funding information The work is jointly funded by the National Key Research and Development Program of China (2016YFA0600303) and the National Natural Science Foundation of China (41375075).

References

- Bao X, Zhang F, Sun J (2011) Diurnal variations of warm-season precipitation east of the Tibetan Plateau over China. *Mon Weather Rev* 139:2790–2810
- Chen G, Sha W, Iwasaki T, Ueno K (2009) Diurnal variation of precipitation over southeastern China: spatial distribution and its seasonality. *J Geophys Res Atmos* 114:D13103
- Chen H, Yuan W, Li J, Yu R (2012a) A possible cause for different diurnal variations of warm season rainfall as shown in station observations and TRMM 3B42 data over the southeastern Tibetan plateau. *Adv Atmos Sci* 29:193–200
- Chen G, Sha W, Iwasaki T, Ueno K (2012b) Diurnal variation of rainfall in the Yangtze River Valley during the spring-summer transition from TRMM measurements. *J Geophys Res Atmos* 117:D06106
- Dee DP, Uppala SM, Simmons AJ, Berrisford P, Poli P, Kobayashi S, Andrae U, Balmaseda MA, Balsamo G, Bauer P, Bechtold P, Beljaars ACM, van de Berg L, Bidlot J, Bormann N, Delsol C, Dragani R, Fuentes M, Geer AJ, Haimberger L, Healy SB, Hersbach H, Hólm EV, Isaksen I, Kållberg P, Köhler M, Matricardi M, McNally AP, Monge-Sanz BM, Morcrette JJ, Park BK, Peubey C, de Rosnay P, Tavolato C, Thépaut JN, Vitart F (2011) The ERA-interim reanalysis: configuration and performance of the data assimilation system. *Q J R Meteorol Soc* 137:553–597
- Gungle B, Krider EP (2006) Cloud-to-ground lightning and surface rainfall in warm-season Florida thunderstorms. *J Geophys Res Atmos* 111:D19203
- He H, Zhang F (2010) Diurnal variations of warm-season precipitation over northern China. *Mon Weather Rev* 138:1017–1025
- Hyun Y-K, Kar S, Ha K-J, Lee J (2010) Diurnal and spatial variabilities of monsoonal CG lightning and precipitation and their association with the synoptic weather conditions over South Korea. *Theor Appl Climatol* 102:43–60
- Klingaman NP, Woolnough S, Syktus J (2013) On the drivers of inter-annual and decadal rainfall variability in Queensland, Australia. *Int J Climatol* 33:2413–2430
- Landin MG, Bosart LF (1989) The diurnal variation of precipitation in California and Nevada. *Mon Weather Rev* 117:1801–1816
- Li D, Sun J, Fu S, Wei J, Wang S, Tian F (2016) Spatiotemporal characteristics of hourly precipitation over central eastern China during the warm season of 1982–2012. *Int J Climatol* 36:3148–3160
- Liu LY, Ma ZG (2013) Intra-annual variability of diurnal cycle precipitation over China from 1960–2000. *Atmos Oceanic Sci Lett* 6:451–456
- Liu C, Zipser EJ (2008) Diurnal cycles of precipitation, clouds, and lightning in the tropics from 9 years of TRMM observations. *Geophys Res Lett* 35:L04819
- Mandapaka P, Germann U, Panziera L (2013) Diurnal cycle of precipitation over complex Alpine orography: inferences from high-resolution radar observations. *Q J R Meteorol Soc* 139:1025–1046
- Qian T, Zhao P, Zhang F, Bao X (2015) Rainy-season precipitation over the Sichuan basin and adjacent regions in southwestern China. *Mon Weather Rev* 143:383–394
- Rouault M, Roy SS, Balling RC (2013) The diurnal cycle of rainfall in South Africa in the austral summer. *Int J Climatol* 33:770–777
- Roy SS, Balling RC (2014) Spatial patterns of diurnal lightning activity in southern Africa during austral summer. *Atmos Res* 145:182–188
- Siderius C, Hellegers P, Mishra A, van Ierland E, Kabat P (2014) Sensitivity of the agroecosystem in the Ganges basin to inter-annual rainfall variability and associated changes in land use. *Int J Climatol* 34:3066–3077
- Tang Y, Gu J, Yu S, Zhang H, He H (2011) Analysis on characteristics of diurnal variation of precipitation in the southwest. *Plateau Meteorol* 30:376–384 (in Chinese)
- Tapia A, Smith JA, Dixon M (1998) Estimation of convective rainfall from lightning observations. *J Appl Meteorol* 37:1497–1509
- Tucker DF (1993) Diurnal precipitation variations in south-central New Mexico. *Mon Weather Rev* 121:1979–1991
- Wallace JM (1975) Diurnal variations in precipitation and thunderstorm frequency over the conterminous United States. *Mon Weather Rev* 103:406–419
- Wang F, Yu R, Chen H, Li J, Yuan W (2011) Analysis on the characteristics of diurnal variation of precipitation in southwest China. *Torrential Rain Disaster* 30:117–121 (in Chinese)
- Wang F, Cao J, Li F, Sun X, Gu X, Xiong W, Duan R (2015) Climatic characteristics of precipitation days at different grades in Guizhou and its relationship with precipitation. *Plateau Meteorol* 34:145–154 (in Chinese)
- Xue Y, Bai A, Li D (2012) Analysis on diurnal variation characteristics of precipitation in Sichuan Basin and case simulation. *Adv Earth Science* 27:885–894
- Yu R, Zhou T, Xiong A, Zhu Y, Li J (2007) Diurnal variations of summer precipitation over contiguous China. *Geophys Res Lett* 34:L01704
- Yu R, Li J, Chen H, Yuan W (2014a) Progress in studies of the precipitation diurnal variation over contiguous China. *Acta Meteor Sinica* 28:877–902
- Yu R, Li J, Chen H, Yuan W (2014b) Research progress of diurnal variation of precipitation in China. *Acta Meteor Sinica* 72:948–968
- Yuan W, Yu R, Chen H, Li J, Zhang M (2010) Subseasonal characteristics of diurnal variation in summer monsoon rainfall over central eastern China. *J Clim* 23:6684–6695
- Yuan W, Sun W, Chen H, Yu R (2014) Topographic effects on spatiotemporal variations of short-duration rainfall events in warm season of central North China. *J Geophys Res Atmos* 119:11223–11234
- Zhang Y, Zhang F, Sun J (2014) Comparison of the diurnal variations of warm-season precipitation for East Asia vs. North America downstream of the Tibetan Plateau vs. the Rocky Mountains. *Atmos Chem Phys* 14:10741–10759
- Zhao Y, Xu M, Wang Y, Xu G, Cui C (2012) Analysis of diurnal variation characteristics of convective precipitation in middle Yangtze River in flood season. *J Guizhou Meteor* 38:1196–1206 (in Chinese)
- Zhuo H, Zhao P, Zhou T (2014) Diurnal cycle of summer rainfall in Shandong of eastern China. *Int J Climatol* 34:742–750